This is a preprint, the final version is subject to change, of the American Mineralogist (MSA)
Cite as Authors (Year) Title. American Mineralogist, in press.
DOI: https://doi.org/10.2138/am-2020-7146

Revision 1

XANES Spectroscopy of Sulfides Stable under Reducing Conditions

Brendan A. Anzures[1], Stephen W. Parman[1], Ralph E. Milliken[1], Antonio Lanzirotti[2], Matthew Newville[2]

[1]Department of Earth and Planetary Sciences, Brown University, Providence, RI 02912 USA

[2]Center for Advanced Radiation Sources, The University of Chicago, Argonne, IL 60439, USA

Corresponding author: first and last name (brendan_anzures@brown.edu)

This is a preprint, the final version is subject to change, of the American Mineralogist (MSA)
Cite as Authors (Year) Title. American Mineralogist, in press.
DOI: https://doi.org/10.2138/am-2020-7146

Abstract

X-ray absorption near-edge structure (XANES) spectroscopy is a powerful technique to quantitatively investigate sulfur speciation in geologically complex materials such as minerals, glasses, soils, organic compounds, industrial slags, and extraterrestrial materials. This technique allows non-destructive investigation of the coordination chemistry and oxidation state of sulfur species ranging from sulfide (2- oxidation state) to sulfate (6+ oxidation state). Each sulfur species has a unique spectral shape with a characteristic K-edge representing the $s \rightarrow p$ and *d hybridization* photoelectron transitions. As such, sulfur speciation is used to measure the oxidation state of samples by comparing the overall XANES spectra to that of reference compounds. Although many S XANES spectral standards exist for terrestrial applications under oxidized conditions, new sulfide standards are needed to investigate reduced (oxygen fugacity, fO_2, below IW) silicate systems relevant for studies of extraterrestrial materials and systems. Sulfides found in certain meteorites (e.g., enstatite chondrites and aubrites) and predicted to exist on Mercury, such as CaS (oldhamite), MgS (niningerite), and $FeCr_2S_4$ (daubréelite), are stable at fO_2 below IW-3 but rapidly oxidize to sulfate and/or produce sulfurous gases under terrestrial surface conditions. XANES spectra of these compounds collected to date have been of variable quality, possibly due to the unstable nature of certain sulfides under typical (e.g., oxidizing) laboratory conditions. A new set of compounds were prepared for this study and their XANES spectra are analyzed for comparison with potential extraterrestrial analogs. S K-edge XANES spectra were collected at Argonne National Lab for FeS (troilite), MnS (alabandite), CaS(oldhamite), MgS (niningerite), $Ni_{1-x}S$, NiS_2, $CaSO_4$ (anhydrite), $MgSO_4$, $FeSO_4$, $Fe_2(SO_4)_3$, $FeCr_2S_4$ (daubréelite), Na_2S, Al_2S_3, Ni_7S_6, and Ni_3S_2; the latter five were analyzed for the first time using XANES. These standards expand upon the existing S XANES endmember libraries at

a higher spectral resolution (0.25 eV steps) near the S K-edge. Processed spectra, those that have been normalized and 'flattened', are compared to quantify uncertainties due to data processing methods. Future investigations that require well-characterized sulfide standards such as the ones presented here may have important implications for understanding sulfur speciation in reduced silicate glasses and minerals with applications for the early Earth, Moon, Mercury, and enstatite chondrites.

Keywords: XANES spectroscopy, chemical state of S, oxidation state of S, sulfides, sulfates, endmember variability.

Introduction

Along with iron, sulfur is the most important heterovalent element in geologic systems. Due to its range of charges from 2- to 6+, the behavior of sulfur is complex. Under different redox conditions, sulfur can bond with both more electropositive and more electronegative elements in magmas, soils, industrial glasses and slags, and meteorites (Fleet 2005). This has significant effects on the partitioning behaviors of these elements between silicate melts (S^{2-} and S^{6+}), liquid metals and sulfides (S^0 and S^{2-}), gases (H_2S, S_2, SO_2, and SO_3), and solids (S^{2-}, S^{1-}, S^0, S^{2+}, S^{4+}, and S^{6+}). Under reducing conditions inferred for enstatite chondrite and aubrite meteorite parent bodies, as well as for lunar and Mercurian magmas, sulfur is stable as a number of different sulfide compounds not typically found on Earth, and S is the most abundant volatile element dissolved in silicate melts (>1 wt%). Sulfides stable below IW-3 include CaS (oldhamite), MgS (niningerite), MnS (alabandite), $FeCr_2S_4$ (daubréelite), $NaCr_2S_2$ (caswellsilverite), and djerfisherite ($K_6Na(Fe^{2+},Cu,Ni)_{25}S_{26}Cl$), all of which rapidly oxidize to sulfate and/or produce sulfurous gases in air under terrestrial surface conditions.

Reduced silicate systems have applications for terrestrial mid-ocean ridge basalt (MORB), meteorites such as enstatite chondrites and aubrites, and magmas on the Moon and Mercury. Mercury is the most extreme example with surface sulfur detections of 1.5-4 wt% (Nittler et al. 2011). Recent work on sulfide solubility in experimental Mercurian glasses (Namur et al. 2016b) predicts MgS and CaS should be the dominant sulfides in extremely reduced silicate melts, while our analyses of sulfide speciation have confirmed and quantified MgS and CaS in reduced S-rich and Fe-poor silicate melts. Therefore, sulfur speciation is critical to understanding the thermodynamics of these sulfur-rich silicate systems and has been shown to influence silicate phase equilibria (Namur et al. 2016b, 2016a) and physical properties such as density, polymerization, and viscosity (Holzheid and Grove 2002; Robert A. Fogel 2005; Namur et al. 2016b).

Sulfur speciation can be determined through a number of spectroscopic techniques including x-ray emission and absorption spectroscopy, nuclear magnetic resonance (NMR), Raman spectroscopy, and Infrared spectroscopy (Wilke et al. 2011). XANES is advantageous because sulfur oxidation state and individual species can be determined quantitatively at concentrations down to ~100 ppm with ~1 micrometer spot size. The XANES analyses can also be compared with spectra estimated by *ab initio* methods (Fleet 2005).

X-ray Absorption Spectroscopy (XAS) works by absorbing x-ray photons into a core orbital level followed by photoelectron emission at a characteristic energy. The resultant spectra can be loosely divided into two main energy regions, X-ray Absorption Near Edge Structure (XANES) and Extended Absorption Fine Structure (EXAFS) that are shown in an example spectrum of MgS (niningerite) in **Figure S1**. XANES is the region within ~50 eV of the absorption edge representing a Fermi level transition, which in this case is the primary S K-edge

corresponding to the photoelectron transition S 1*s* → 3*p*. Secondary absorption peaks shown in the near-edge structure may result from transitions to empty S 3*d* states or hybridization of S *p* states with metal 3*d* states (i.e. Mg) (Fleet 2005). EXAFS is the oscillatory region ~30eV above the absorption edge that probes the local environment of atoms. For light elements such as S, the information EXAFS can provide is limited because the oscillatory structure decays rapidly to a line past the edge (e.g. Bunker & Stern, 1984; Fleet, 2005). For a more detailed overview of the theory and practice of S XANES see Fleet (2005) and references therein.

A number of sulfur species standards have been analyzed in previous studies, including FeS (troilite), MnS, CaS, MgS, $Ni_{1-x}S$, NiS_2, $CaSO_4$ (anhydrite), $MgSO_4$, $FeSO_4$, and $Fe_2(SO_4)_3$ (e.g. Fleet, 2005; Langman et al., 2015). These data indicate that the S K-edge moves to higher energies as the sulfide bonding environment shifts from metallic/covalent to ionic, and from reduced (S^{2-}) to oxidized (S^{6+}) species as seen in **Figure 1.** Here, a new set of S XANES standards for sulfide and sulfate compounds were synthesized. By protecting the samples from air throughout synthesis, transport, and analysis, these standards are expected to be stoichiometrically stable during high-precision spectral measurements. S K-edge XANES measurements were made at beamline 13-IDE at Argonne National Lab, which is tunable to 0.25 eV spectral resolution in the energy range of sulfur with a focused beam resolution of ~1 μm. New S K-edge XANES spectra are presented for FeS (troilite), MnS (alabandite), CaS(oldhamite), MgS (niningerite), $Ni_{1-x}S$, NiS_2, $CaSO_4$ (anhydrite), $MgSO_4$, $FeSO_4$, $Fe_2(SO_4)_3$, $FeCr_2S_4$ (daubréelite), Na_2S, Al_2S_3, Ni_7S_6, and Ni_3S_2. Below, we also present the range in processed XANES spectra that can result from different choices in data processing steps and discuss how the resulting variations translate to uncertainties in the final processed spectra of the S standards. This type of endmember spectral variability has been extensively studied for remote

sensing applications of reflectance spectroscopy over the past several decades (Tompkins et al. 1997; Settle 2006; Somers et al. 2011), and it is similarly important to understand how uncertainties associated with processing of XANES data propagate through spectral unmixing of such data for multi-component mixtures (e.g., materials with multiple S-bearing phases).

Methods

Experimental Methods

Pure sulfides were synthesized by reaction of element powders or purchased from Alfa Aesar©. MgS (niningerite) was synthesized from Mg metal powder and excess S powder in a sealed evacuated silica tube following the method of Osborne & Fleet (1984). Mg was reacted with S at 600 °C for 1 day and 700 °C for 2 days. The product was then crushed and reloaded with excess S in a 15 cm long silica tube with the reagents located in the hotspot of the horizontal furnace at 700 °C for 1 day and 900 °C for 1 day. Crushing and reloading decreases the effect of armoring that limits reaction progress. FeS (troilite) was synthesized from Fe metal powder and S powder at stochiometric proportions in a sealed evacuated silica tube held at 800 °C for 48 hours. NiS_2 (vaesite), $Ni_{1-x}S$, Ni_7S_6, and Ni_3S_2 (heazlewoodite) was synthesized from Ni metal powder or Ni metal rod and S powder at stochiometric proportions in a sealed evacuated silica tube similarly held at 800 °C for 48 hours. $FeCr_2S_4$ (daubréelite) was synthesized from reagent grade powders in experimental Mercurian samples at *T*s >1250 °C and 1GPa for 24 hours in a piston cylinder apparatus at Brown University. The Mercurian sample composition was a modified CH chondrite composition ALH85085 (Weisberg et al. 1988). CaS (oldhamite), Na_2S, MnS (alabandite), and Al_2S_3 of >99.9% purity were purchased from Alfa Aesar©.

Fe, $FeCr_2S_4$, Ni_{1-x}, Ni_7S_6, and Ni_3S_2 were mounted in epoxy and polished under water using steps of 600 and 1200 grit sandpaper, and 0.5 and 0.03 micrometer Al_2O_3 grit. All other sulfides were kept in powder form. All sulfides were stored and transported in a nitrogen filled desiccator to minimize potential reaction with oxygen and water.

Analytical Methods

Experimental sulfide compositions were confirmed using the Cameca SX100 electron microprobe (EMPA) or by powder x-ray diffraction (XRD) using a Bruker D2 Phaser instrument. For EMPA analyses, metals were used as Ti, Mn, Ni, Cr, and Fe standards, while diopside was used as the Ca and Si standard. Forsterite was used as the Mg standard. Pyrite was used as the S standard. Synthesized sulfides were analyzed using a 15 keV accelerating voltage, a 10 nA beam current, and a 1 μm spot size. Based on repeated analyses, purity is >95% for MgS (~5% MgO) and $FeCr_2S_4$ (<5% Mn) and >99% for FeS, NiS_2, $Ni_{1-x}S$, Ni_7S_6, and Ni_3S_2 with relative errors less than 0.5%. MgS (niningerite) was left in powdered form to prevent oxidation during any subsequent sample preparation and thus analyzed using XRD. No sulfate peaks were detected in the XRD or XANES data during repeated analyses.

S K-edge XANES spectra were collected inside a helium environment using an undulator-based, hard x-ray microprobe at beamline 13IDE of GSECARS, Argonne National Laboratory. The spot size for XANES spectroscopy was 1-2 micrometers, with a nominal penetration depth of 2-3 micrometers for S. XANES spectra were collected from 2442 to 2542 eV with a step size of 0.25 eV near the S K-edge and 2 eV in the other energy regions (1 s acquisition time per step).

Data Processing Methods

Processing of XANES spectra included converting raw data to values of absorption coefficient (μ(E)). S K-edge XANES spectra were calibrated with the white line maxima energy for FeS (troilite) at 2470.30 eV, CaS at 2474.30 eV, MgS at 2473.60 eV, $CaSO_4$ (anhydrite) at 2481.90 eV, and $MgSO_4$ at 2481.70 eV. Dead-time corrections were completed at APS. XANES spectra were deglitched in Athena to remove anomalous data points associated with Bragg spots and irregular x-ray input energies (Ravel and Newville 2005). Additionally, the spectra for Al_2S_3 were smoothed to reduce the noise in the data using a 3-point boxcar average. These steps account for analytical, instrument, and facility errors and uncertainty. Two steps, normalization and flattening, can be applied to XANES spectra. Although these steps are common in spectral processing, they require input from the user and can thus be a source of uncertainty in the absolute values of the final spectra. We evaluate and discuss below how these user inputs may affect the final processed spectra of our S-bearing samples.

Spectra were normalized using an edge step normalization algorithm that fits the energy region before the K-edge and the energy region after the edge using separate linear regressions (Ravel & Newville, 2005), as shown in **Figure S1**. The raw data is subtracted by the pre-edge

curve and then divided by the edge-step, where the edge step is the difference between the post-edge curve and pre-edge curve at E0. E0 is a parameter that represents the k=0 continuum level at which electrons have just enough energy to propagate through material. Normalization of XANES spectra allows data to be directly compared regardless of the details of the experiment by regularizing the effects of sample preparation, sample thickness, absorber concentration, and detector and amplifier settings (Ravel & Newville, 2005). Normalization operates to remove the pre-edge background by setting the absorption intensity values in the pre-edge region to 0 and to scale data to a per-atom basis by scaling the edge jump to 1. Example raw and normalized spectra for MgS (niningerite) and CaS (oldhamite) are shown in **Figure 2**.

Flattening is an optional processing step after normalization that scales the absorption values in the EXAFS region (oscillatory part of the data after the absorption edge) to be near the y=1 line, thus minimizing the spectral slope at post-edge energies. To 'flatten' a XANES spectrum, the normalized spectrum is subtracted by the difference between the normalized post-edge curve and normalized edge-step at E0, where E0 is calculated as the first inflection point on the absorption edge.

XANES normalization optimization allows one to quantify the uncertainty introduced in the processed spectra when choosing pre-edge and post-edge normalization bounds. Once quantified, the uncertainty that results from this processing step may be incorporated into weighted linear combination fits of spectra of multicomponent samples, and this may be particularly important if spectra of potential endmember components exhibit K-edge positions that are close to one another. During normalization and flattening there are 4 free parameters (referred to here as PER1, PER2, NR1, and NR2), excluding E0. PER1 and PER2 represent the energy positions that define the bounds of the spectral data that are used in the linear regression

of the pre-edge region (Figure S1). Similarly, NR1 and NR2 define the energy bounds of the spectral data that is fit in the linear regression of the post-edge region (Figure S1). During spectral normalization and flattening, the bounds of the pre-edge were varied for PER1 and PER2 between the lowest-energy value of the spectrum plus 5 eV and E0-14:-4 in steps of 1 eV respectively. The bounds of the post-edge, NR1 and NR2, were allowed to vary between E0+5:30 and the highest-energy value of the spectrum minus 10 eV in steps of 1 eV respectively. This resulted in 29766 unique combinations of input parameters and thus 29766 processed XANES spectra per sample.

Results

Normalization Optimization

Normalization and flattening of XANES spectra are deemed to be satisfactory when they remove the pre-edge background by setting the pre-edge region to 0 and scale the edge jump to 1, allowing direct comparison of spectra. As shown in **Figure 3**, there are a number of possible solutions for the linear regressions to the pre- and post-edge regions depending on the range of range of data chosen for the fit (i.e., positions of PER1, PER2, NR1, and NR2). However, it is logical to take the furthest points (PER1 and NR2) along with middle points that allow the fit to bisect data spread within the spectral region of interest. In the pre-edge case, the middle point would preferably be before any pre-edge or K-edge absorption feature. In the post-edge case, the middle point would be any point that allows the EXAFS region to be bisected by the fit (which may be many as the EXAFS region is characterized by its oscillatory nature). Good normalization has a convergent solution with minimal error and effect on spectral shape as determined by slope and RMSE of the pre-edge and edge-step regions. Good normalizations were determined by setting the tolerance of the edge-step to between 0.95 and 1.05, the pre-edge

RMSE below 0.3, and the pre-edge slope desired to be y=0. The top ten and best normalizations were chosen by ranking the processed spectra based on root mean square error of the pre-edge slope, pre-edge RMSE, and edge-step RMSE. The full range, reduced range (top 10), and best normalized and flattened spectra are shown in **Figure 3a and 4b.**

Spectra of New Sulfur Standards

New S K-edge XANES standards were collected for a number of S species including FeS, MgS, CaS, MnS, $Ni_{1-x}S$, NiS_2, $CaSO_4$ (anhydrite), $MgSO_4$, $FeSO_4$, and $Fe_2(SO4)_3$, $FeCr_2S_4$ (daubréelite), Na_2S, and Al_2S_3, Ni_7S_6, and Ni_3S_2. All S species XANES spectra are shown as normalized spectra in **Figure 4**, **Figure 5**, and **Figure 6** with flattened spectra in **Figures S2 and Figure S3**. Unlike sulfite and sulfate species, sulfides with different cations display characteristic XANES spectra K-edge energies and shapes (**Table 1**). XANES spectra of MnS, $Ni_{1-x}S$, NiS_2 and $CaSO_4$ are comparable to previous measurements (e.g. Fleet, 2005) except FeS (troilite), CaS (oldhamite), and MgS (niningerite) all have lower K-edge energies. The primary K-edge of FeS, CaS, and MgS are measured at 2469.3(1) eV, 2471.2(1) eV, and 2472.0(1) eV compared to 2470.0 eV, 2474.0 eV, and 2475.1 eV respectively (Fleet 2005). Additionally, we find MgS has 3 resolvable K-edge peaks instead of just the 2 present in the data of Fleet (2005), highlighting the advantage of higher spectral resolution data (**Figure 1** compared to **Figure 4**). Spectra of FeS (troilite) and Na_2S exhibit similar K-edge energy of 2469.3 eV indicating the Na-S bond is very metallic. A weak sulfate peak at 2482 eV is observed in the CaS and Na_2S spectra, likely due to their rapid reactivity in air to form trace amounts of sulfate (**Figure 4**). The XANES spectrum of $FeCr_2S_4$ (daubréelite) is very similar to that of pure FeS (troilite) (**Figure 4)**, which suggests the structure and bonding environments of Fe and Cr are very similar. All nickel sulfides exhibit

similar spectra with no systematic trend in K-edge position or peak strength due to differing Ni/S ratios (**Figure 5**).

Discussion

S XANES K-edge Location

The location of the S K-edge and overall shape of the XANES spectra depends on the cation, bond character, and bonding environment. Sulfide species with low-lying empty 3d orbitals (transition metal sulfides including Fe, Ni, and Cr sulfides) have an initial absorption peak due to hybridization of the S antibonding and metal 3*d* states and a second broad absorption peak corresponding to transitions to S *p*-like states hybridized with the metal 4*sp* orbitals (Farrell and Fleet 2001; Farrell et al. 2002b; Kravtsova et al. 2004; Soldatov et al. 2004; Fleet 2005) as shown in **Figures 4 and 5**. Sulfide species with bonds that are more covalent/metallic are expected to have lower K-edges than those with ionic bonds (Fleet 2005). S K-edge energy increases as the ionic character of the bond increases (Pauling 1960) showing a linear trend for monosulfides with a cation charge of 2+ in **Figure 7**. Nickel disulfide has a higher K-edge energy due to higher mean oxidation state of the sulfur atom relative to the nickel monosulfide similar to FeS_2 compared with FeS (Head et al. 2018). However, bond length and structural effects also influence the K-edge energy influencing the nickel sulfide trends for monoclincic ($Ni_{1-x}S$), orthorhombic (Ni_7S_6), isometric (NiS_2), and trigonal (Ni_3S_2) nickel sufides (Fleet 1972). As the oxidation state of S increases (2- for sulfides to 6+ for sulfates), the energy of the S K-edge increases as well (Li et al. 1995; Fleet 2005) (**Table 1)**. Ultimately, the K-edge energy of the S species correlates linearly with an increase in the direct energy-band gap (Li et al. 1994).

XANES Normalization

The chief aim of normalization, whether or not a spectrum is subsequently flattened, is to regularize data to allow for direct comparison of different samples measured under different conditions. The three main methods of normalization are functional normalization, edge-step normalization, and flattening. Edge-step normalization is used here to avoid issues of inverted regions of a functional normalized spectrum due to division by negative background absorption possibly arising from detector settings (Ravel and Newville 2005). Unfortunately edge-step normalization can introduce a small amount of attenuation that is linear with energy and quadratic in wavenumber, but does represent a much less severe issue than functional normalization because it does not invert portions of a spectrum (Ravel and Newville 2005).

As expected, normalized spectra exhibit higher variance in the post-edge EXAFS region (standard error ≈ 0.005-0.01 for normalized and standard error ≈ 0.001-0.01 for flattened), whereas the flattened spectra exhibit higher variance in the pre-edge XANES region (standard error ≈ 0.00001-0.001 for normalized and standard error ≈ 0.01-0.05 for flattened) as shown in **Figure 3c and 3d** with standard errors reported in supplementary tables. Variance is still highest at the K-edge and near-edge structure (standard error ≈ 0.01-0.02 for sulfides and standard error ≈ 0.01-0.05 for sulfates). Although flattened spectra can be beneficial for displaying the data and linear combination fitting (Webb 2005), it does inherently introduce processing error into the pre-edge region. Thus, we recommend using edge-step normalized XANES spectra for XANES spectroscopy deconvolution studies, especially if pre-edge features are important in the spectral fits. Nevertheless, K-edge position is insensitive to the choice of the processing parameters; the K-edge is found to vary by 0.1 eV for all sulfides and less than 0.3 eV for all sulfates as seen in **Table 1**.

Implications

X-ray absorption near-edge structure (XANES) spectroscopy is an excellent technique to non-destructively investigate sulfur speciation regardless of sample type for both geologic and industrial applications. S K-edge XANES spectra are presented for FeS, $FeCr_2S_4$ (daubréelite), MgS, CaS, MnS, Na_2S, Ni_7S_6, Ni_3S_2, $Ni_{1-x}S$, NiS_2, Al_2S_3, $CaSO_4$ (anhydrite), $MgSO_4$, $FeSO_4$, and $Fe_2(SO4)_3$. These new endmember spectra will be especially useful in deconvolving reduced silicate glasses that may be dominated by (Mg,Ca)S (Robert A Fogel 2005; Stockstill-Cahill et al. 2012; Namur et al. 2016b) and other sulfides stable under reducing conditions rather than FeS. While this represents an important expansion of the existing S XANES endmember library, more analyses of S-bearing phases are needed. It is of interest to measure alkali sulfides such as caswellsilverite ($NaCrS_2$) and djerfisherite ($K_6Na(Fe^{2+},Cu,Ni)_{25}S_{26}Cl$) that are common in reduced enstatite chondrites but difficult to synthesize in pure forms. Fortunately, XANES analyses of sulfide solid solutions have shown that the S K-edge peaks vary with local cation environment (or average cation environment) in structurally similar sulfides to their constituent parts as long as the proportion of Fe remains the same (Farrell and Fleet 2001; Farrell et al. 2002a). S K-edge XANES spectra for solid solutions of (Mn,Fe)S and (Mg,Fe)S have shown that the pre-edge peak area does not increase proportional to increasing Fe and progressive participation of 3*d* orbitals in metal-S bonding (Farrell et al. 2002a). Also, because the structure is factored into the multiple scattering and resultant spectra, one might think that synthesizing and measuring structurally similar endmembers (glass vs. crystalline) would improve deconvolution fits of spectra of complex mixtures. In fact, some electron microprobe standards have been developed for both crystalline and glassy materials. In the future, MgS dissolved in enstatite or forsterite glass could improve deconvolution of silicate glass XANES spectra. In addition, questions remain as to whether there is a normalization algorithm that minimizes

uncertainties due to spectral processing methods across the entire spectrum. The spectral uncertainty measured for these new sulfur standards and presented here will also be useful in determining how endmember variability affects quantitative spectral unmixing of XANES spectra of materials containing multiple S-bearing phases. These new sulfide standards should improve future studies of sulfur speciation in reduced silicate glasses and minerals in both industrial and geologic contexts, with applications for the early Earth, Moon, Mercury, and enstatite chondrites.

Acknowledgements

We acknowledge the experimental and analytical facilities at Brown University and GeoSoilEnviroCars (Sector 13), Advanced Photon Source, Argonne National LaboratoryThis research used resources of the Advanced Photon Source, a U.S. Department of Energy (DOE) Office of Science User Facility operated for the DOE Office of Science by Argonne National Laboratory under Contract No. DE-AC02-06CH11357. We acknowledge the funding of NASA grant No. NNX15AH63G and NASA Earth and Space Sciences fellowship No. 80NSSC18K1245.

References

Bunker, G., and Stern, E.A. (1984) Experimental Study of Multiple Scattering in X-Ray-Absorption Near-Edge Structure. Physical Review Letters, 52, 13–16.

Farrell, S.P., and Fleet, M.E. (2001) Sulfur K-edge XANES study of local electronic structure in ternary monosulfide solid solution [(Fe, Co, Ni)0.923S]. Physics and CHemistry of Minerals, 28, 17–27.

Farrell, S.P., Fleet, M.E., Stekhin, I.E., Kravtsova, A.N., Soldatov, A. V., and Liu, X. (2002a)

318 Evolution of local electronic structure in alabandite and niningerite solid solutions
319 [(Mn,Fe)S, (Mg,Mn)S, (Mg,Fe)S] using sulfur K- and L-edge XANES spectroscopy.
320 American Mineralogist, 87, 1321–1332.

321 Farrell, S.P., Stekhin, I., and Soldatov, A. (2002b) In situ analysis of the formation steps of the
322 gold nanoparticles synthesis View project XANES spectroscopy : shape resonances and
323 multiple scattering final states View project. American Mineralogist, 87, 1321–1332.

324 Fleet, M.E. (1972) The crystal structure of α-Ni7S6. Acta Crystallographica Section B, 28,
325 1237–1241.

326 Fleet, M.E. (2005) XANES spectroscopy of sulfur in Earth materials. Canadian Mineralogist, 43,
327 1811–1838.

328 Fogel, Robert A. (2005) Aubrite basalt vitrophyres: The missing basaltic component and high-
329 sulfur silicate melts. Geochimica et Cosmochimica Acta, 69, 1633–1648.

330 Fogel, Robert A (2005) Aubrite basalt vitrophyres: The missing basaltic component and high-
331 sulfur silicate melts.

332 Head, E.M., Lanzirotti, A., Newville, M., and Sutton, S. (2018) Vanadium, sulfur, and iron
333 valences in melt inclusions as a window into magmatic processes: A case study at
334 Nyamuragira volcano, Africa. Geochimica et Cosmochimica Acta, 226, 149–173.

335 Holzheid, A., and Grove, T.L. (2002) Sulfur saturation limits in silicate melts and their
336 implications for core formation scenarios for terrestrial planets. American Mineralogist, 87,
337 227–237.

338 Kravtsova, A.N., Stekhin, I.E., Soldatov, A. V., Liu, X., and Fleet, M.E. (2004) Electronic
339 structure of MS (M = Ca , Mg , Fe , Mn) : X-ray absorption analysis. Physical Review B,

69, 134109.

Langman, J.B., Blowes, D.W., Veeramani, H., Wilson, D., Smith, L., Sego, D.C., and Paktunc, D. (2015) The mineral and aqueous phase evolution of sulfur and nickel with weathering of pyrrhotite in a low sulfide, granitic waste rock. Chemical Geology, 401, 169–179.

Li, D., Bancroft, G.M., Kasrai, M., Fleet, M.E., Feng, X.H., Yang, B.X., and Tan, K.H. (1994) S K- and L-edge XANES and electronic structure of some copper sulfide minerals, 317–324 p. Physics and Chemistry of Minerals Vol. 21.

Li, D., Bancroft, G.M., Kasrai, M., and Fleet, M.E. (1995) S K- And L-edge X-ray absorption spectroscopy of metal sulfides and sulfates: applications in mineralogy and geochemistry. The Canadian Mineralogist, 33, 949–960.

Namur, O., Collinet, M., Charlier, B., Grove, T.L., Holtz, F., and Mccammon, C. (2016a) Melting processes and mantle sources of lavas on Mercury. Earth and Planetary Science Letters, 439, 117–128.

Namur, O., Charlier, B., Holtz, F., Cartier, C., and Mccammon, C. (2016b) Sulfur solubility in reduced mafic silicate melts: Implications for the speciation and distribution of sulfur on Mercury. Earth and Planetary Science Letters, 448, 102–114.

Nash, W.M., Smythe, D.J., and Wood, B.J. (2019) Compositional and temperature effects on sulfur speciation and solubility in silicate melts. Earth and Planetary Science Letters, 507, 187–198.

Nittler, L.R., Starr, R.D., Weider, S.Z., McCoy, T.J., Boynton, W. V., Ebel, D.S., Ernst, C.M., Evans, L.G., Goldsten, J.O., Hamara, D.K., and others (2011) The major-element composition of Mercury's surface from MESSENGER X-ray spectrometry. Science, 333,

1847–1850.

Osborne, M.D., and Fleet, M.E. (1984) Mossbauer Investigation of Niningerite Solid Solutions (Mg , Fe) S. Physics and Chemistry of Minerals, 10, 245–249.

Pauling, L. (1960) The Nature of the Chemical Bond and the Structure of Molecules and Crystals: An Introduction to Modern Structural Chemistry. Cornell university press, Ithaca, NY.

Ravel, B., and Newville, M. (2005) Ravel and Newville ¯ Data analysis for XAS using IFEFFIT computer programs J. Synchrotron Rad, 12, 537–541.

Settle, J. (2006) On the effect of variable endmember spectra in the linear mixture model. IEEE Transactions on Geoscience and Remote Sensing, 44, 389–396.

Soldatov, A. V., Kravtsova, A.N., Fleet, M.E., and Harmer, S.L. (2004) Electronic structure of MeS (Me = Ni, Co, Fe): x-ray absorption analysis. J. Phys.: Condens. Matter, 16, 7545–7556.

Somers, B., Asner, G.P., Tits, L., and Coppin, P. (2011) Endmember variability in Spectral Mixture Analysis: A review. Remote Sensing of Environment, 115, 1603–1616.

Stockstill-Cahill, K.R., McCoy, T.J., Nittler, L.R., Weider, S.Z., and Hauck, S.A. (2012) Magnesium-rich crustal compositions on mercury: Implications for magmatism from petrologic modeling. Journal of Geophysical Research E: Planets, 117.

Tompkins, S., Mustard, J.F., Pieters, C.M., and Forsyth, D.W. (1997) Optimization of Endmembers Mixture Analysis for Spectral. Science Inc, 59, 472–489.

Webb, S.M. (2005) SIXPack a Graphical User Interface for XAS Analysis Using IFEFFIT. Physica Scripta, 2005, 1011.

Weisberg, M.K., Prinz, M., and Nehru, C.E. (1988) Petrology of ALH85085: a chondrite with unique characteristics. Earth and Planetary Science Letters, 91, 19–32.

Wilke, M., Klimm, K., and Kohn, S.C. (2011) Spectroscopic Studies on Sulfur Speciation in Synthetic and Natural Glasses. Reviews in Mineralogy and Geochemistry, 73, 41–78.

List of figure captions

Figure 1. S K-edge energy depends on the coordination chemistry and oxidation state of S for the compound. The S K-edge moves to higher energies as the bonding environment shifts from metallic/covalent to ionic and from reduced (S^{2-}) to oxidized (S^{6+}) species. The dashed line indicates E0 of the compound.

Figure 2. S XANES spectra of MgS (niningerite) and CaS (oldhamite) showing a) raw data and b) normalized data. Raw XANES spectra may differ in background (pre-edge level), absorption (near-edge peaks) that is nonlinearly proportional to concentration, and energy-dependent decay (post-edge). Normalized XANES spectra of different samples with different concentrations and sample form can be directly compared and used in linear combination fitting of mixed spectra.

Figure 3. Normalization optimization of CaS (oldhamite) S K-edge XANES spectra. a) Normalized and b) flattened spectra showing the full range (n=29766) in red as well as the best according to the optimization program in black. Variance of the full range for c) normalized and d) flattened data generally follow the shape of the data but have error introduced in either the c) post-edge or d) pre-edge regions. Normalized data is better to compare the XANES region, while flattened data is better to compare the EXAFS region.

Figure 4. Normalized Sulfur K-edge XANES spectra for reference compounds and minerals. $Ni_{1-x}S$, FeS (troilite), MnS (alabandite), CaS (oldhamite), MgS (niningerite), and $CaSO_4$ (anhydrite) spectra are comparable to previous studies (e.g. Fleet, 2005), however MgS has three near-edge peaks as opposed to two seen in Fleet (2005). $FeCr_2S_4$, Na_2S, and Al_2S_3 were measured for the first time. The dashed line indicates E0 of the compound. The spectra were collected in total fluorescence yield.

Figure 5. Normalized Sulfur K-edge XANES spectra for nickel sulfides. $Ni_{1-x}S$ is comparable to Fleet (2005). The S K-edge moves to higher energies in progression of $Ni_{1-x}S$, Ni_7S_6, Ni_3S_2, to NiS_2. The dashed line indicates E0 of the compound. The spectra were collected in total fluorescence yield.

Figure 6. Normalized Sulfur K-edge XANES spectra for sulfates. Unlike sulfides, sulfates do not have significant variation in the S K-edge energy with bonding cation ($CaSO_4$, $MgSO_4$, and $FeSO_4$) or oxidation state ($FeSO_4$ and $Fe_2(SO_4)_3$. There does appear to be a small peak at ~2478 for $FeSO_4$ that has been attributed to some degree of photo-reduction in previous analyses (Nash et al. 2019). The dashed line indicates E0 of the compound. The spectra were collected in total fluorescence yield.

Figure 7. Position of S K-Edge for reference compounds show the general relationship of increasing S K-Edge energy with increasingly ionic (as opposed to covalent/metallic) bond behavior calculated as percent ionic character (Pauling, 1960). Monosulfides with 2+ cation

charge (filled circles: $Ni_{1-x}S$, FeS, MnS, MgS, CaS) show a linear trend. Monosulfides with different cation charges (open circles: Ni_7S_6, Ni_3S_2, NiS_2, Al_2S_3, Na_2S) are also shown. Daubréelite (cross: $FeCr_2S_4$) percent ionic character was calculated using a Cr-S bond. The marker size corresponds to the K-edge uncertainty of 1 eV for all sulfides.

Tables

Table 1. Position of S K-edge peaks in some sulfur species

Mineral or compound	K-edge energy (eV)	Mineral or compound	K-edge energy (eV)
$FeCr_2S_4$ (daubréelite)	2469.0(1)	Al_2S_3	2471.9(1)
FeS (troilite)	2469.4(1)	$Ni_{1-x}S$	2469.0(1)
Na_2S	2469.2(1)	Ni_7S_6	2469.4(1)
MnS (alabandite)	2470.6(1)	NiS_2 (vaesite)	2470.3(1)
	2471.8(1)	Ni_3S_2 (heazlewoodite)	2470.2(1)
	2473.2(1)	$CaSO_4$ (anhydrite)	2480.5(1)
CaS (oldhamite)	2471.5(1)	$MgSO_4$	2480.7(3)
	2474.1(1)	$Fe_2(SO4)_3$	2480.9(2)
MgS (niningerite)	2472.2(1)	$FeSO_4$	2481.3(1)
	2473.3(1)		
	2475.0(1)		

Figures

This is a preprint, the final version is subject to change, of the American Mineralogist (MSA)
Cite as Authors (Year) Title. American Mineralogist, in press.
DOI: https://doi.org/10.2138/am-2020-7146

Figure 1

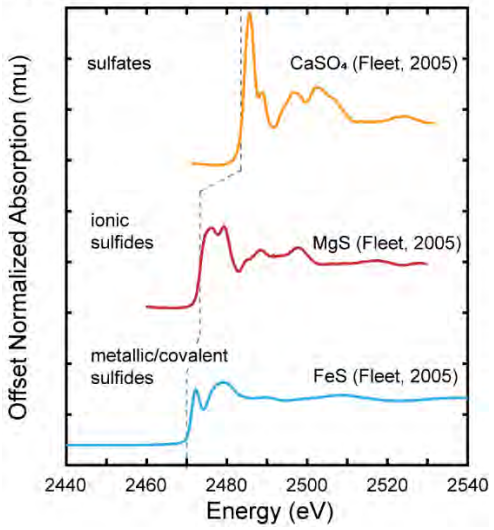

Figure 2

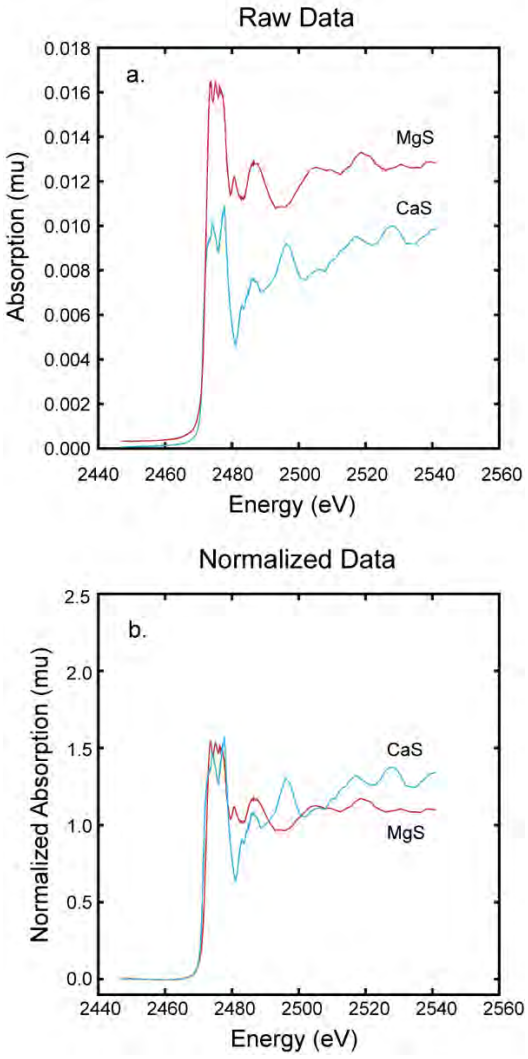

This is a preprint, the final version is subject to change, of the American Mineralogist (MSA)
Cite as Authors (Year) Title. American Mineralogist, in press.
DOI: https://doi.org/10.2138/am-2020-7146

Figure 3

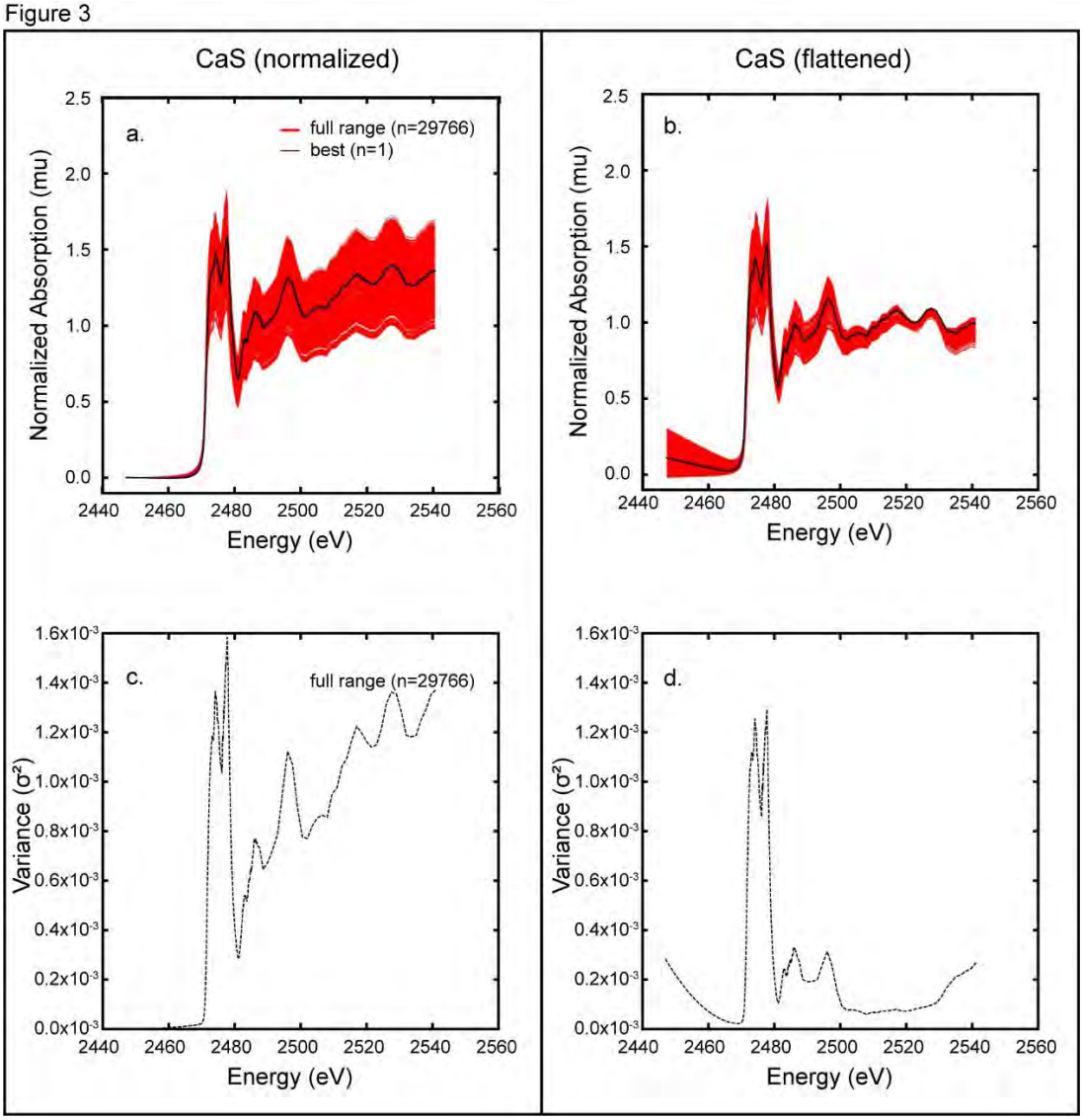

442

Figure 4

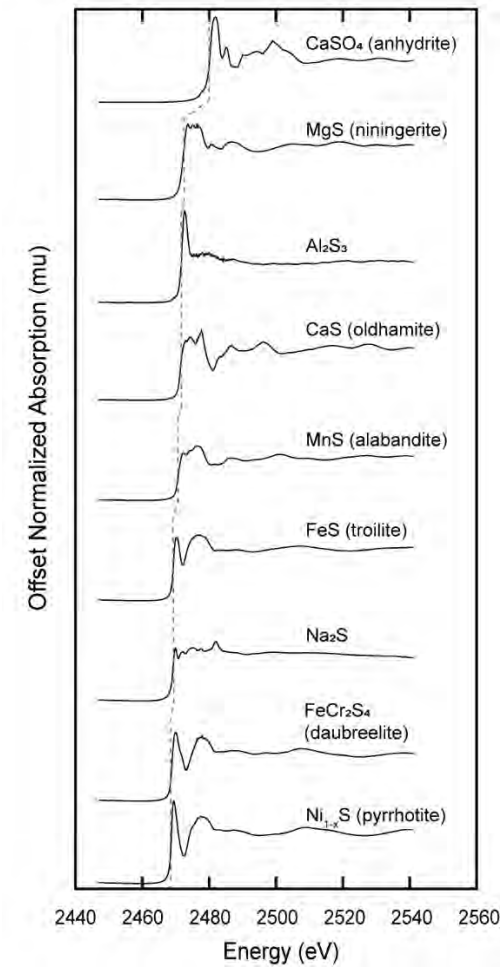

443

Figure 5

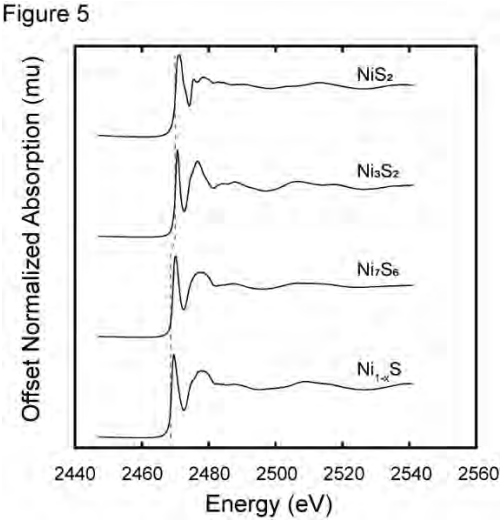

444

Figure 6

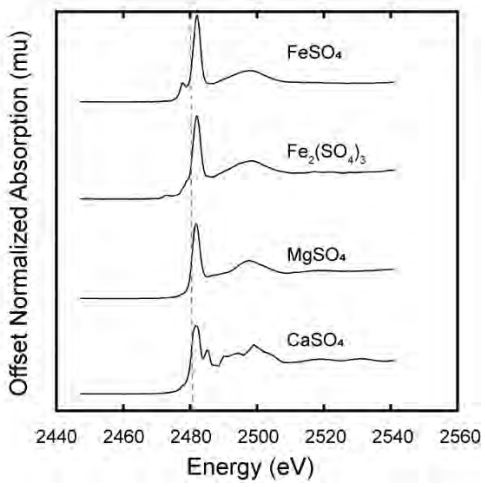

445

Figure 7

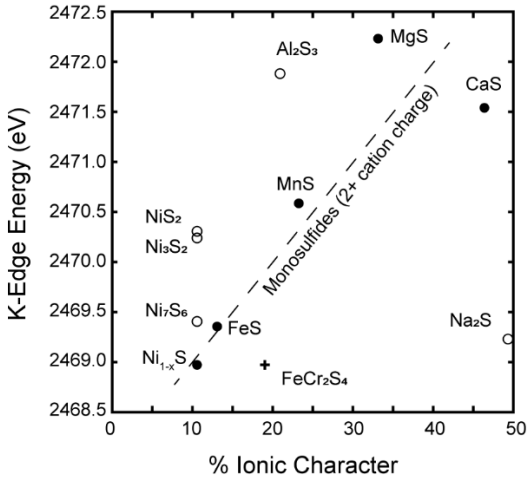

446